THE ASTROPHYSICAL JOURNAL, 494:409–418, 1998 February 10
© 1998. The American Astronomical Society. All rights reserved. Printed in U.S.A.

WEAKLY COMPRESSIBLE MAGNETOHYDRODYNAMIC TURBULENCE IN THE SOLAR WIND AND THE INTERSTELLAR MEDIUM

A. BHATTACHARJEE, C. S. NG, AND S. R. SPANGLER
Department of Physics and Astronomy, University of Iowa, Iowa City, IA 52242
Received 1997 February 20; accepted 1997 September 4

ABSTRACT

A new four-field system of equations is derived from the compressible magnetohydrodynamic (MHD) equations for low Mach number turbulence in the solar wind and the interstellar medium, permeated by a spatially varying magnetic field. The plasma beta is assumed to be of order unity or less. It is shown that the full MHD equations can be reduced rigorously to a closed system for four fluctuating field variables: magnetic flux, vorticity, pressure, and parallel flow. Although the velocity perpendicular to the magnetic field is shown to obey a two-dimensional incompressibility condition (analogous to the Proudman-Taylor theorem in hydrodynamics), the three-dimensional dynamics exhibit the effects of compressibility. In the presence of spatial inhomogeneities, the four dynamical equations are coupled to each other, and pressure fluctuations enter the weakly compressible dynamics at leading order. If there are no spatial inhomogeneities and or if the plasma beta is low, the four-field equations reduce to the well-known equations of reduced magnetohydrodynamics (RMHD). For pressure-balanced structures, the four-field equations undergo a remarkable simplification which provides insight on the special nature of the fluctuations driven by these structures. The important role of spatial inhomogeneities is elucidated by 2.5-dimensional numerical simulations. In the presence of inhomogeneities, the saturated pressure and density fluctuations scale with the Mach number of the turbulence, and the system attains equipartition with respect to the kinetic, magnetic, and thermal energy of the fluctuations. The present work suggests that if heliospheric and interstellar turbulence exists in a plasma with large-scale, nonturbulent spatial gradients, one expects the pressure and density fluctuations to be of significantly larger magnitude than suggested in nearly incompressible models such as pseudosound.

Subject headings: ISM: general — MHD — plasmas — solar wind — turbulence

1. INTRODUCTION

Magnetohydrodynamics (MHD), despite its significant limitations as a model, provides the principal framework for the theoretical description of turbulence in the solar wind and the interstellar medium (ISM). Since the observed fluctuations involve density variations, it is widely appreciated that the effects of plasma compressibility should be incorporated ab initio, in the theory. However, theoretical attempts to grapple with compressible turbulence from first principles are hampered by the formidable analytical (as well as numerical) complexities of the fully compressible MHD equations which involve eight scalar variables (i.e., three components each for the fluid velocity and magnetic fields, the plasma density, and pressure) and several nonlinearities. Recent numerical studies have included the effect of compressibility but have done so with simplifying assumptions regarding the geometry of the background magnetic field. These include studies of compressible MHD turbulence in the solar wind (Roberts, Ghosh, & Goldstein 1996; Malara, Primavera, & Veltri 1996), ISM, and molecular clouds (Passot, Vázquez-Semadini, & Pouquet 1995; Gammie & Ostriker 1996). Despite the assumptions regarding geometry, these studies have succeeded in including a substantial number of relevant physical effects and have illuminated significant aspects of a complex reality.

MHD turbulence is characterized by a multiplicity of space and timescales. In a mean-field theory, every dynamical variable can be thought of as an algebraic sum of a mean and a fluctuation, with distinct spatial and temporal characteristics. The mean quantities are generally characterized by slow variations in space and time, whereas fluctuations vary on more rapid space and timescales. This separation of space and timescales between mean and fluctuating quantities, when it exists, can be exploited in the development of a self-consistent dynamical theory. If the system is closed, then the mean and the fluctuations (in steady state) are strongly interdependent. However, if the system is open, as is the case for most astrophysical plasmas, there may be external factors that also influence the mean properties of the system. In such open systems, the mean properties determine the physical nature of internal turbulent fluctuations, but the converse may not be true. In the absence of complete information on the mean properties of a given system, a reasonable approach is to use the available information on mean properties to constrain the theory as much as possible and then determine the nature and properties of turbulent fluctuations.

Although the mean properties of plasmas in the solar wind and the interstellar medium (ISM) are not completely known, they are often characterized by three qualitative features: there is a mean magnetic field, the plasma beta (β) is less than or of the order unity, and the spatial inhomogeneities of the mean quantities are of order of the system size or less. The main goal of this paper is to present a new system of equations for MHD turbulence with these distinguishing features. We show from first principles that the fully compressible, three-dimensional MHD equations can be simplified to a four-field system (i.e., involving four scalar variables) for the fluctuation dynamics. The four scalar variables are the magnetic flux, the parallel vorticity (i.e., the component of vorticity parallel to the mean magnetic field), the perturbed pressure, and the parallel flow. The four-field system does provide some computational economy when compared with the fully compressible equations, but not nearly as much as the well-known reduced magnetohydrodynamic (RMHD) system (Rosenbluth et al. 1976; Strauss 1976; Zank & Matthaeus 1992) for $\beta \ll 1$ plasmas. The RMHD equations have been very successful in modeling nonlinear and turbulent phenomena in low-beta systems such as tokamaks and the solar corona. In a way, the four-field system may be reviewed as the first nontrivial generalization of RMHD (a two-field system) to plasmas with $\beta \leq 1$. We show below that the four-field system is useful not only because it offers some computational economy but, more significantly, because it offers insights on how to distinguish between different dynamical features of compressible MHD turbulence.

In § 2, we present the four-field equations and discuss a question of conceptual importance: do the effects of plasma compressibility enter the fluctuation dynamics at leading order for $\beta \sim 1$ plasmas, or are the effects of compressibility a higher-order phenomenon enslaved to a leading-order incompressible description? In the most general case with spatial inhomogeneities in the mean magnetic field and plasma pressure, we demonstrate that the effects of plasma compressibility do enter the dynamical equation for the pressure fluctuation at leading order, and that the four-field variables are irreducibly coupled. In this case, our leading-order equations differ significantly with the RMHD or nearly incompressible MHD equations proposed by Zank & Matthaeus (1992, hereafter ZM). We consider two special cases when the four-field system decouples to yield the two-field equations of RMHD: (1) when the mean magnetic field is constant in space and all spatial inhomogeneities in the mean-field quantities are neglected, and/or (2) when $\beta \ll 1$. While these special cases may apply to specific numerical experiments or to a selected set of observations, they are much too idealized to be of general relevance for the solar wind and the ISM. We also consider pressure-balanced structures and show that the four-field equations undergo a remarkable simplification to a system slightly more general than RMHD. Thus, turbulence associated with pressure-balanced structures can be described quite naturally as a special case of the four-field model.

In § 3, we present numerical results based on the four-field equations, contrasting them with RMHD. We illustrate these differences in the context of a physical example involving current sheet dynamics and turbulence due to the interaction of a periodic array 2.5-dimensional coronal flux tubes. Spatial inhomogeneities are shown to play a qualitatively important role in determining the nature of small-scale dynamics as well as the efficiency with which root mean square (rms) pressure fluctuations attain equipartition with the magnetic and kinetic energy of the fluctuations. In § 4, we conclude with a summary and the implications of our results for observations in the solar wind and the ISM.

2. COMPRESSIBLE MHD EQUATIONS AND SCALING

The compressible resistive MHD equations are

$$\rho\left(\frac{\partial}{\partial t} + \boldsymbol{v} \cdot \nabla\right)\boldsymbol{v} = -\nabla p + \frac{1}{4\pi}(\nabla \times \boldsymbol{B}) \times \boldsymbol{B} , \qquad (1)$$

$$\frac{\partial \boldsymbol{B}}{\partial t} + \nabla \times (\boldsymbol{B} \times \boldsymbol{v} + \eta c \boldsymbol{J}) = 0 , \qquad (2)$$

$$\frac{\partial \rho}{\partial t} + \nabla \cdot (\rho \boldsymbol{v}) = 0 , \qquad (3)$$

$$\frac{d}{dt}\left(\frac{p}{\rho^{\gamma}}\right) = \frac{\gamma - 1}{\rho^{\gamma}} \eta |\boldsymbol{J}|^2 , \qquad (4)$$

where ρ is the plasma density, $\boldsymbol{v}$ is the fluid velocity, p is the plasma pressure, $\boldsymbol{B}$ is the magnetic field, $\boldsymbol{J} = c\nabla \times \boldsymbol{B}/4\pi$ is the current density, c is the speed of light, η is the plasma resistivity, and γ is the ratio of specific heats. Equation (4) is written under the assumption that Joule heating is the only relevant non-adiabatic process. This assumption can be relaxed to include radiative heating and cooling which are often important processes in the ISM. We cast equations (1)–(4) in dimensionless form by scaling every dependent variable by its characteristic (constant) value, designated by a subscript c (which should not be confused with the speed of light). We define the sound speed, Alfvén speed, Mach number, Alfvén Mach number, and the plasma beta, respectively, by the relations

$$C_s^2 = (\partial p/\partial \rho)_c , \qquad (5a)$$

$$V_{\mathrm{A}}^2 \equiv B_c^2/4\pi\rho_c , \qquad (5b)$$

$$M^2 \equiv v_c^2/C_s^2 , \qquad (5c)$$

$$M_{\mathrm{A}}^2 \equiv v_c^2/V_{\mathrm{A}}^2 , \qquad (5d)$$

$$\beta \equiv 4\pi\rho_c/B_c^2 = M_{\mathrm{A}}^2/\gamma M^2 . \qquad (5e)$$

In terms of scaled (dimensionless) variables, equations (1), (2), and (4) can be written

$$\rho\left(\frac{\partial}{\partial t} + \boldsymbol{v} \cdot \nabla\right)\boldsymbol{v} = \frac{1}{\epsilon^2}\left(-\nabla p + \frac{1}{\beta}(\nabla \times \boldsymbol{B}) \times \boldsymbol{B}\right), \qquad (6a)$$

$$\frac{\partial \boldsymbol{B}}{\partial t} + \nabla \times (\boldsymbol{B} \times \boldsymbol{v} + \eta \boldsymbol{J}) = 0 , \qquad (6b)$$

$$\frac{d}{dt}\left(\frac{p}{\rho^{\gamma}}\right) = \frac{\gamma - 1}{\beta\rho^{\gamma}} \eta |\boldsymbol{J}|^2 , \qquad (6c)$$

where $\epsilon \equiv \gamma^{1/2}M$, with $\boldsymbol{J} = \nabla \times \boldsymbol{B}$, and equation (3) retains its present form. (Distance and time are scaled by the system size and the Alfvén time, respectively.) Since equations (1)–(4) are invariant under Galilean transformations, we choose to work in a reference frame that is stationary with respect to the plasma. The parameter ϵ, which is essentially the Mach number of the turbulence, is assumed to be much smaller than one and provides the basis for an asymptotic expansion of the dependent variables. We write

$$\boldsymbol{B} = \boldsymbol{B}_0 + \boldsymbol{B}_1 + \cdots , \quad \boldsymbol{v} = \boldsymbol{v}_1 + \cdots ,$$

$$\rho = \rho_0 + \rho_1 + \cdots , \quad p = p_0 + p_1 + \cdots , \qquad (7)$$

where all $O(1)$ quantities are denoted by subscript zero and $O(\epsilon)$ quantities by the subscript one. We have assumed that if there is a large-scale flow of the plasma, it is uniform and can be transformed away by moving to the plasma frame (i.e., $\boldsymbol{v}_0 = 0$).

Near equilibrium, we obtain to leading order from equation (6a),

$$\nabla p_0 = \frac{1}{\beta}(\nabla \times \boldsymbol{B}_0) \times \boldsymbol{B}_0 , \qquad (8)$$

where gradients of all mean quantities, as the quantities themselves, are taken to be $O(1)$. ZM claim (over restrictively) that in order for the compressible equations to have bounded time derivatives, the zeroth-order solutions must satisfy

$$p_0 = 1 \ , \quad \boldsymbol{B}_0 = \hat{z} \ , \tag{9}$$

which is a special solution of equation (8). We shall consider the special case equation (9) later, but propose to develop our model with more general solutions of equation (8) in mind, allowing for the presence of spatial inhomogeneities.

In the next section, we discuss the four-field equations for the fluctuation dynamics. These equations were published by Bhattacharjee & Hameiri (1988) 10 years ago for studies of resistive fluid turbulence in reversed-field pinches, but the authors were then unaware of the possible relevance of these equations to astrophysical plasmas. Also, the original derivation was couched in the specific ordering of resistive pressure-driven instabilities, and their more general validity for low Mach number turbulence was not transparent. Nonetheless, after we implement the new ordering discussed above, it turns out that the equations derived in § 3 are identical to those obtained by Bhattacharjee & Hameiri. This is an illustration of the "principle of maximal balance (or minimal simplification)" in asymptotics, articulated by Kruskal, according to which the "... most widely applicable and most informative ordering is that which simplifies the least, maintaining a maximal set of comparable terms" (Kruskal 1963). Thus, two superficially different ordering procedures yield the same equations because both retain a maximum number of comparable terms (for $\beta \sim 1$ plasmas) in the nonlinear MHD equations.

3. THE FOUR-FIELD EQUATIONS

The form of equations (6a) and (8) motivate the transformations $\boldsymbol{B} \to \beta^{1/2}\boldsymbol{B}$, $\boldsymbol{J} \to \epsilon\beta^{1/2}\boldsymbol{J}$, $\eta \to \eta/\epsilon^2$, $\boldsymbol{v} \to \boldsymbol{v}/\epsilon$, $\nabla \to \epsilon\nabla$, so that $\boldsymbol{B} \sim O(1/\beta^{1/2})$, $\boldsymbol{v} \sim O(\epsilon)$, and $\nabla \sim O(1/\epsilon)$. Under these transformations, equations (6a) and (8) become

$$\rho\left(\frac{\partial}{\partial t} + \boldsymbol{v} \cdot \nabla\right)\boldsymbol{v} = -\nabla p + (\nabla \times \boldsymbol{B}) \times \boldsymbol{B} \ , \tag{10}$$

and

$$\nabla p_0 = (\nabla \times \boldsymbol{B}_0) \times \boldsymbol{B}_0 \ , \tag{11}$$

respectively. Also, equations (3) and (4) may be combined to yield

$$\frac{\partial p}{\partial t} + \boldsymbol{v} \cdot \nabla p + \gamma p \nabla \cdot \boldsymbol{v} = (\gamma - 1)\eta \, |\boldsymbol{J}|^2 \ . \tag{12}$$

Under these transformations, equation (6b) remains the same, while equation (6c) becomes equation (4), with $\boldsymbol{J} = \nabla \times \boldsymbol{B}$.

In many turbulent plasmas of practical interest, the spatial and temporal derivatives of mean and fluctuating quantities (indicated, respectively, by the subscripts zero and one in eq. [7]) are often significantly different. Specifically, fluctuations tend to vary much more rapidly in space and time than mean quantities. The asymptotic ordering described below reflects these differences.

Due to the presence of a large-scale magnetic field $\boldsymbol{B}_0$, the fluctuations will exhibit slow spatial variation parallel to $\boldsymbol{B}_0$ but rapid variation perpendicular to $\boldsymbol{B}_0$. To represent this behavior, we decompose the gradient operator acting on fluctuations into parallel and perpendicular components with the ordering $\nabla_\parallel \sim O(1)$ and $\nabla_\perp \sim O(1/\epsilon)$, respectively. In contrast, when the gradient operator acts on mean quantities, we impose the ordering $\nabla \sim O(1)$.

Fluctuations tend to vary with time more rapidly than mean quantities. We assume that $\partial/\partial t \sim O(1)$ for fluctuations but $\partial/\partial t \sim O(\epsilon^2)$ for mean quantities. The latter assumption is consistent with the derivation of equation (12) and ensures that the pressure-balance condition (eq. [11]) continues to hold as the (first-order) fluctuations evolve in time. [Note that this ordering implies that for a mean quantity f_0 and a fluctuation f_1, we have $\partial f_0/\partial t \sim O(\epsilon^2)$ whereas $\partial f_1/\partial t \sim O(\epsilon)$.]

From the requirement $\nabla \cdot \boldsymbol{B} = 0$ since $\nabla \cdot \boldsymbol{B}_0 = 0$, we obtain to $O(1)$

$$\nabla_\perp \cdot \boldsymbol{B}_1 = 0 \ . \tag{13}$$

From the momentum equation (10), we obtain to $O(\epsilon^2)$,

$$p_1 + \boldsymbol{B}_0 \cdot \boldsymbol{B}_1 = 0 \ . \tag{14}$$

Equation (14) is identical to equation (47) of Zank & Matthaeus (1993). It implies that the parallel component of the magnetic field fluctuation is proportional to the pressure fluctuation. By equations (13) and (14), we write

$$\boldsymbol{B}_1 = \nabla_\perp A \times \boldsymbol{b} - p_1 \boldsymbol{b} \ , \tag{15}$$

where $\boldsymbol{b} \equiv \boldsymbol{B}_0/B_0^2$ and A is the perturbed flux function.

To $O(1)$, equation (12) yields

$$\nabla_\perp \cdot \boldsymbol{v}_1 = 0 \ . \tag{16}$$

Equation (16) implies that the perturbed flow is incompressible in the (local) two-dimensional plane perpendicular to $\boldsymbol{B}_0$ although it is not incompressible in three dimensions. This is analogous to the well-known Proudman-Taylor theorem in hydrodynamics (see Batchelor 1967). We refer to such flow dynamics as weakly compressible. By equation (16), we write

$$\boldsymbol{v}_1 = \nabla_\perp \phi \times \boldsymbol{b} - v_1 \boldsymbol{b} \ , \tag{17}$$

where ϕ is a stream function and v_1 is the parallel flow. Note that the representation (17) guarantees that the condition (16) is automatically satisfied.

Equations (15) and (17) contain four-field variables: A, p_1, ϕ, and v_1. In the Appendix we demonstrate that the fully compressible resistive MHD equations (1)–(4) can be reduced to the following closed system:

$$\frac{dA}{dt} = \boldsymbol{B}_0 \cdot \nabla\phi + \eta\nabla_\perp^2 A \ , \tag{18}$$

$$\rho_0 \frac{d\Omega}{dt} = DJ + 2\boldsymbol{b} \times \nabla P \cdot \nabla_\perp p_1 - (\boldsymbol{b} \cdot \nabla B_0^2)J \ , \tag{19}$$

$$\frac{dp_1}{dt} = -\boldsymbol{v}_1 \cdot \nabla p_0 + \frac{\gamma p_0}{\gamma p_0 + B_0^2} (2\boldsymbol{v}_1 \cdot \nabla P + Dv_1 + \eta\nabla_\perp^2 p_1) \ , \tag{20}$$

$$\rho_0 \frac{dv_1}{dt} = Dp_1 + \boldsymbol{B}_1 \cdot \nabla p_0 \ . \tag{21}$$

Here

$$\Omega \equiv -\nabla_\perp^2 \phi \,, \tag{22a}$$

$$J \equiv -\nabla_\perp^2 A \,, \tag{22b}$$

$$P \equiv p_0 + B_0^2/2 \,, \tag{22c}$$

$$\frac{d}{dt} \equiv \frac{\partial}{\partial t} + \boldsymbol{v} \cdot \nabla_\perp \,, \tag{22d}$$

$$D \equiv (\boldsymbol{B}_0 + \boldsymbol{B}_{1\perp}) \cdot \nabla \,, \tag{22e}$$

$$\nabla_\perp \equiv \nabla - \hat{\boldsymbol{B}}_0 \hat{\boldsymbol{B}}_0 \cdot \nabla \,, \quad \hat{\boldsymbol{B}}_0 \equiv \boldsymbol{B}_0 / B_0 \,, \tag{22f}$$

$$\rho_0 = p_0^{1/\gamma} \,. \tag{22g}$$

Equations (18)–(21) comprise the four-field system. We repeat for emphasis that the background field satisfies the equilibrium condition (11) and that $\boldsymbol{B}_0$ is generally not spatially uniform. Now in order to make connections with other reduced systems, we consider some special limits. In particular, to see the role of the plasma beta and spatial inhomogeneity, it is convenient to write

$$\boldsymbol{B}_0 = \frac{\hat{\boldsymbol{z}}}{\sqrt{\beta}} + \boldsymbol{B}_s(\boldsymbol{x}) \,. \tag{23}$$

We note:

1. If $\boldsymbol{B}_s(\boldsymbol{x}) \to 0$, then equations (18) and (19) simplify to RMHD with two field variables A and ϕ. Equations (20) and (21) are decoupled from equations (18) and (19) in this limit, and we recover the results of ZM.
2. The case $\beta \ll 1$ is effectively the same as $\boldsymbol{B}_s(\boldsymbol{x}) \to 0$, and conclusion (1) again holds. (This is nothing more than a reconfirmation of RMHD in the $\beta \ll 1$ limit.)

An interesting simplification of the four-field equations occurs if we specialize to pressure-balanced structures, characterized by the relation $P \equiv p_0 + B_0^2/2 =$ constant (cf. Tu & Marsch 1995). Then equations (18) and (19) decouple from equations (20) and (21), but equation (19) contains the additional term $(\boldsymbol{b} \cdot \nabla B_0^2)J$, absent in RMHD. The implication of this simplification is that pressure-balanced structures obey dynamical equations slightly more general than RMHD.

In general, if $\beta \sim 1$ so that $\boldsymbol{B}_s(\boldsymbol{x})$ is large enough, *the effect of compressibility enters the dynamics at leading order and cannot be enslaved to an incompressible flow field.* In this general case, $p_1 \neq 0$ and $\rho_1 \neq 0$ which differs from the predictions of the pseudosound or nearly incompressible models (Montgomery, Brown, & Matthaeus 1987; Matthaeus & Brown 1988; ZM). Due to the dynamical coupling at leading order between the pressure fluctuations and the flow field, brought about by the presence of spatial inhomogeneities, the first-order pressure and density fluctuations, even if they are small initially, can increase to the level of the Mach number. As discussed in § 5, this behavior has significant implications for observations of fluid turbulence in the solar wind and the ISM.

4. 2.5-DIMENSIONAL NUMERICAL SIMULATION

In order to compare four-field MHD turbulence with RMHD turbulence, we present results from a 2.5-dimensional numerical simulation. We represent the (scaled) mean magnetic field as

$$\boldsymbol{B}_0 = \nabla_{\perp 0} A_0(x, y) \times \hat{z} + \hat{z}/\sqrt{\beta} \,, \tag{24}$$

where

$$\nabla_{\perp 0} = \hat{\boldsymbol{x}} \frac{\partial}{\partial x} + \hat{\boldsymbol{y}} \frac{\partial}{\partial y} \,, \tag{25}$$

and $A_0(x, y)$ is the mean flux representing the spatially inhomogeneous component of the mean magnetic field in the $x - y$ plane. From equations (11) and (24) it follows that $p_0 = p_0(A_0)$. If we choose

$$p_0 = 1 + k^2 A_0^2/2 \,, \tag{26}$$

where k is a constant, then A_0 must satisfy the Grad-Shafranov equation:

$$\nabla_{\perp 0}^2 A_0 + dp_0/dA_0 = 0 \,,$$

or

$$\nabla_{\perp 0}^2 A_0 = -k^2 A_0 \,. \tag{27}$$

Assuming periodic boundary conditions in x and y, an exact solution of equation (27) is

$$A_0 = a(\cos 2\pi x - \sin 2\pi y) \,, \tag{28}$$

where we have chosen $k = 2\pi$.

The 2.5-dimensional four-field equations are

$$\frac{\partial A}{\partial t} = -b_z[\phi, A] + [A_0, \phi] + \eta \nabla_\perp^2 A \,, \tag{29a}$$

$$\frac{\partial p}{\partial t} = -b_z[\phi, p + p_0] + \frac{\gamma p_0}{\gamma p_0 + B_0^2} \times \{2b_z[\phi, P] - v\boldsymbol{b} \cdot \nabla B_0^2 + [A_0, v] + b_z[A, v] + \eta \nabla_\perp^2 p\} \,, \tag{29b}$$

$$\rho_0 \frac{\partial \Omega}{\partial t} = -\rho_0 b_z[\phi, \Omega] + 2b_z[p, P] - J\boldsymbol{b} \cdot \nabla B_0^2 + [A_0, J] + b_z[A, J] \,, \tag{29c}$$

$$\rho_0 \frac{\partial v}{\partial t} = -\rho_0 b_z[\phi, v] + b_z[A, p + p_0] + [A_0, p] \,, \tag{29d}$$

where the Poisson bracket $[F, G] \equiv (\partial F/\partial x)(\partial G/\partial y) - (\partial G/\partial x)(\partial F/\partial y)$. (In order to keep the notation simple, we have dropped the subscript unity on all first-order quantities.) Equations (29a)–(29d) display clearly all the coefficients that depend on spatially inhomogeneous mean quantities, which are held fixed for the duration of the computer runs. We apply periodic boundary conditions and represent all dependent field variables in Fourier series, such as

$$\phi(x, y) = \sum_{mn} \phi_{mn} e^{2\pi i(mx + ny)} \,, \tag{30}$$

where m and n are integers. Equations (29a)–(29d) are integrated forward in time by a predictor-corrector method, with the nonlinear terms calculated by finite difference in physical space (see Dahlquist, Björck, & Anderson 1974). For all the runs reported in this paper, the spatial resolution is 256×256.

We hold β at the fixed value one in all the runs. Since the four-field equations have been derived with the ordering $p_0 \le O(1)$, and p_0 is assumed to have the functional form (26), we must constrain the parameter a by the inequality $k^2 A_0^2/2 \le 1$. Since the maximum magnitude of A_0 is $2a$ and $k = 2\pi$, by equation (28) the chosen values of a should be constrained by the inequality $a < 0.1125$. To be consistent with this constraint, we choose $a = 0$, 10^{-6}, 10^{-4}, 10^{-3}, 0.01, 0.04, 0.06, and 0.08 for the runs reported here. Note that a is a measure of the relative magnitude of the spatially

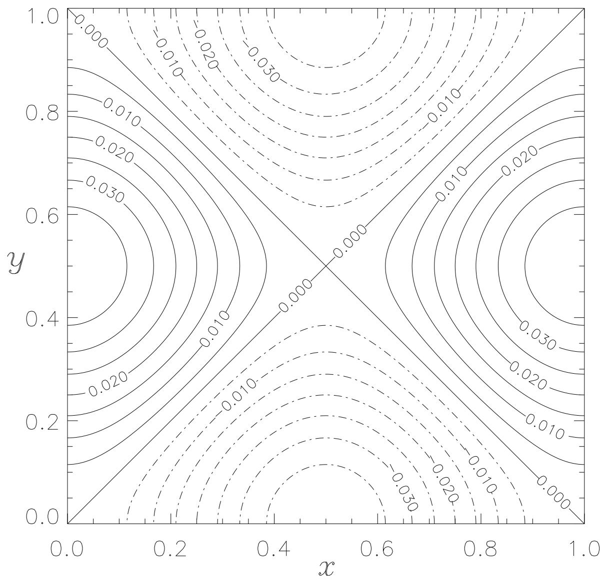

FIG. 1.—Contour plot of the background field A_0 (given by eq. [28]) with $a = 0.04$.

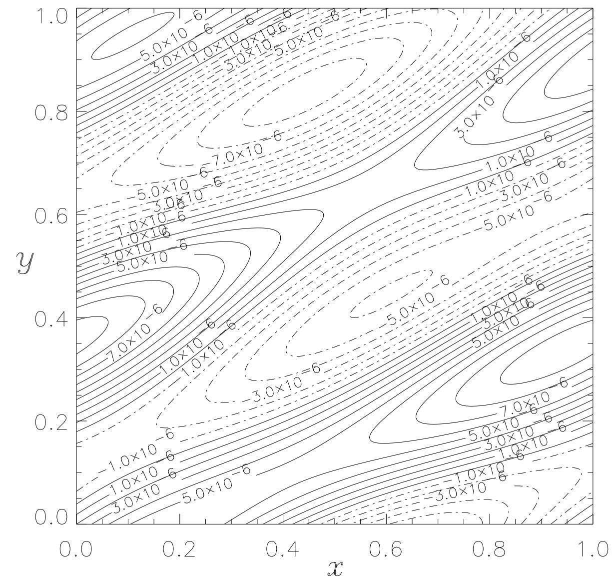

FIG. 3.—Contour plot of the initial flux $A(x, y, t = 0)$ with initial magnetic energy $E_M(t = 0) \approx 3.3 \times 10^{-9}$.

inhomogeneous part of the background magnetic field with respect to the spatially homogeneous part, and k^{-1} is a measure of the characteristic spatial scale of the inhomogeneous magnetic field relative to the system size.

Figure 1 shows a contour plot of level surfaces of the mean flux A_0 on the $x - y$ plane. This is a two-dimensional projection of four flux tubes carrying currents, two parallel and two antiparallel to $\hat{z}$. The tubes are unstable to the coalescence instability which arises from the tendency of two parallel current-carrying tubes to attract each other. The tubes coalesce, squeezing magnetic flux and generating thin current sheets in between them. Due to the presence of finite resistivity, magnetic reconnection occurs at the separatrices, facilitating the process of coalescence.

Most of the runs are initialized with an arbitrarily chosen initial flow field $\phi(x, y, t = 0)$, shown in Figure 2, with kinetic energy $E_K(t = 0) \approx 9.708 \times 10^{-5}$ and initial Mach number $M(t = 0) \approx 0.01$. [Additional data from runs with initial Mach number $M(t = 0) \approx 0.1$ are also shown in Fig. 6 below.] The initial perturbed flux $A(x, y, t = 0)$, shown in Figure 3, corresponds to an initial magnetic energy, $E_M(t = 0) \approx 3.3 \times 10^{-9}$, which is much smaller than the initial flow energy $E_K(t = 0)$. We set $p = v = 0$ at $t = 0$ and carry out a series of runs with the same initial conditions but with different values of the inhomogeneity parameter a. The Lundquist number of these simulations is approximately 10^3.

The results of RMHD are recovered as a smooth limit of four-field MHD when the limit $a \to 0$ is taken. When a is very small ($\leq 10^{-6}$), the overall dynamics of the four-field system is very similar to RMHD dynamics ($a = 0$). However, even with moderate values a ($= 10^{-4}, 10^{-3}$), there

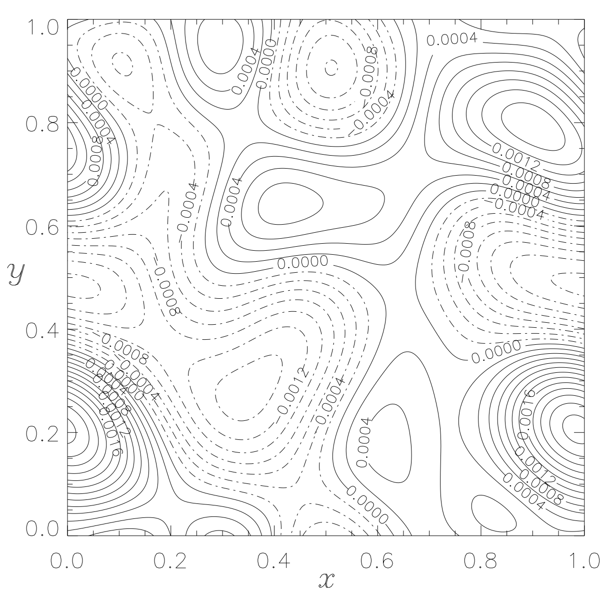

FIG. 2.—Contour plot of the initial flow field $\phi(x, y, t = 0)$, with kinetic energy $E_K(t = 0) \approx 9.708 \times 10^{-5}$ and Mach number $M(t = 0) \approx 0.01$.

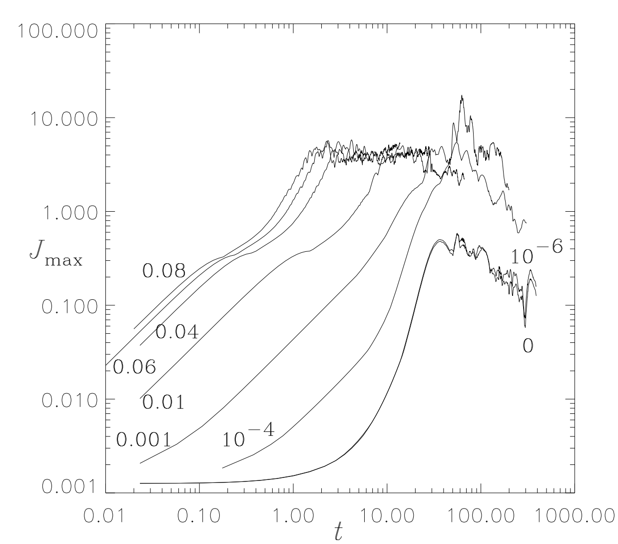

FIG. 4.—Plots of maximum current density, J_{max}, over the whole space vs. time t for different values of a, indicated near each curve.

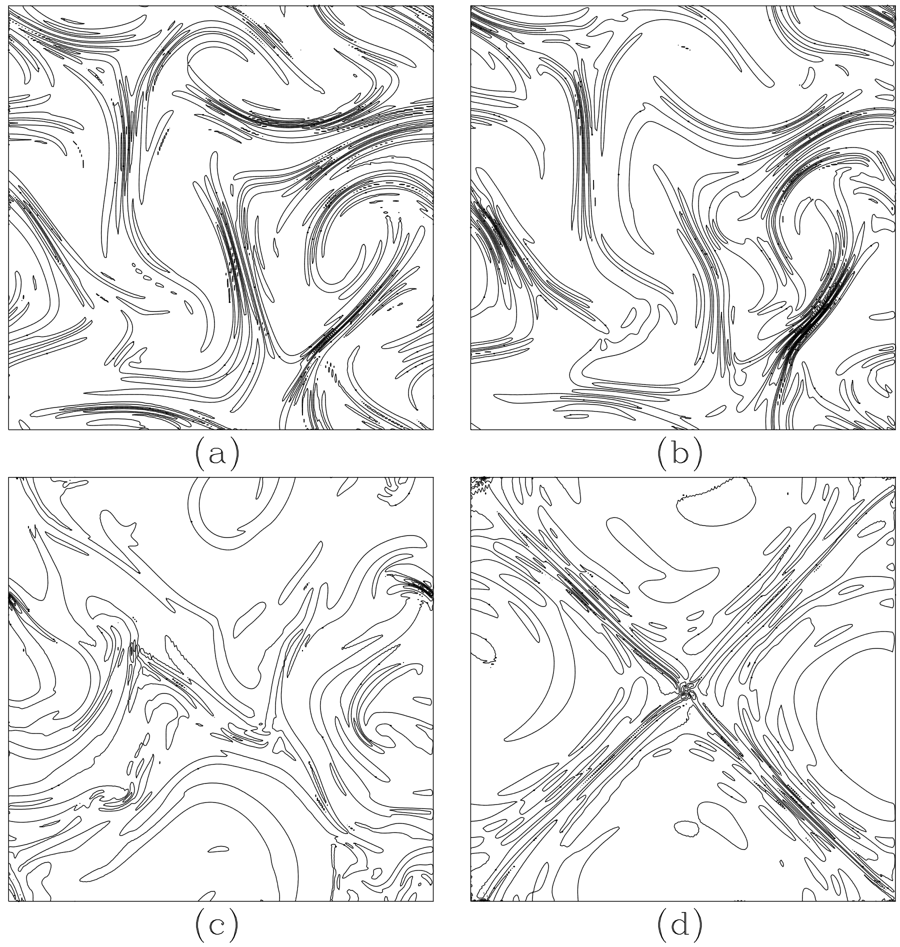

FIG. 5.—Contour plots of current density for different values of a at the time t near the instant when J_{max} attains its highest value (see Fig. 4). (*a*) $a = 10^{-6}$, (*b*) $a = 10^{-4}$, (*c*) $a = 10^{-3}$, (*d*) $a = 10^{-2}$.

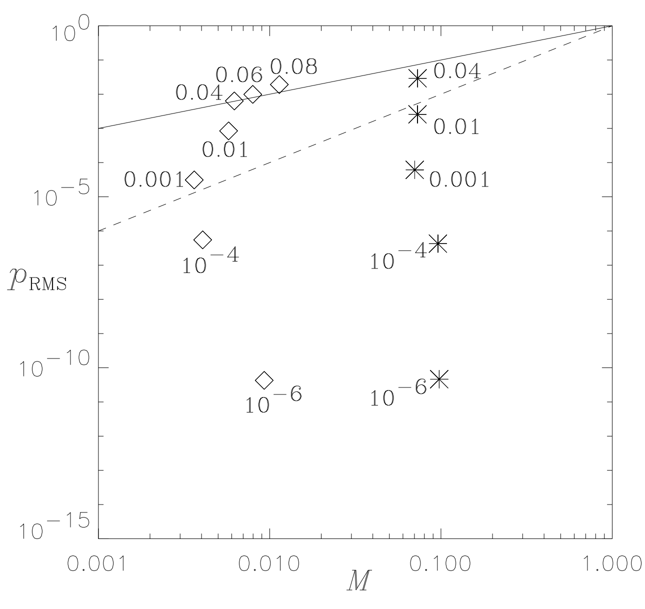

FIG. 6.—Level of the rms value of the first-order pressure p_{rms} in the quasi-saturated state as a function of the Mach number M for different values of a, for $M(t = 0) \approx 0.01$ (*diamonds*) and $M(t = 0) \approx 0.1$ (*stars*). Solid line corresponds to $p_{rms} = M$, and dashed line to $p_{rms} = M^2$.

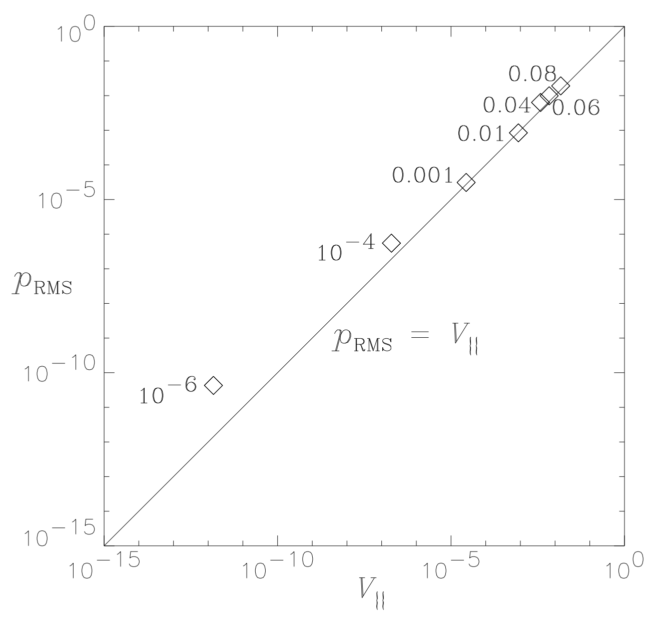

FIG. 7.—Level of p_{rms} in the quasi-saturated state vs. the rms value $V_{\|}$ of the parallel flow $(v_1)_{\|} = -v_1/B_0$ for different values of a. The line $p_{rms} = V_{\|}$ is shown.

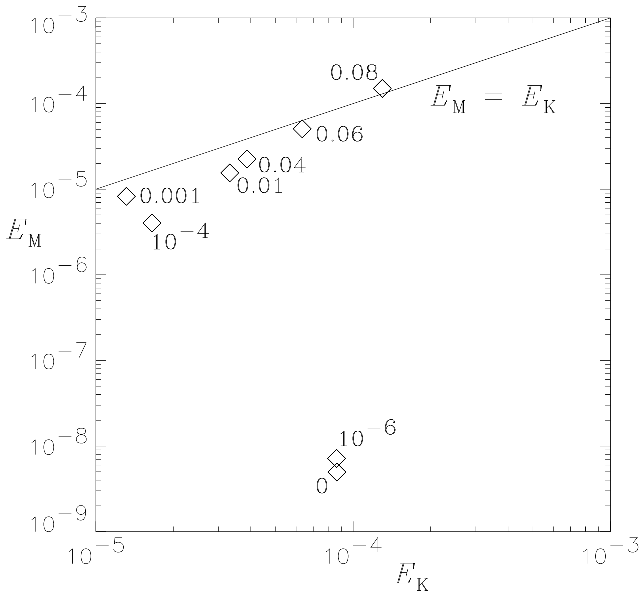

FIG. 8.—Level of magnetic energy E_M vs. kinetic energy E_K in the quasi-saturated state for different values of a. The line $E_M = E_K$ is shown.

are significant dynamical differences between four-field and RMHD dynamics.

Figure 4 shows a plot of the maximum current density versus time for different values of a; we see a more rapid and intense build-up of current density as a increases. As shown in Figure 5, which plots current density contours at the instant of time when the current density attains its highest value, even the dynamic alignment and morphology of thin current sheets change as a increases. For $a = 10^{-6}$ (Fig. 5*a*), thin current sheets develop in localized regions, but they do not appear to have any favored orientation. However, as a increases (Figs. 5*b*–5*d*), the dynamics is increasingly determined by the structure of the mean state. Note that in Figure 5*d* ($a = 0.01$), the thin current sheets are nearly aligned along the diagonal lines in Figure 1. The temporal evolution of these intermittent structures is quite different in four-field and RMHD turbulence. For $a = 0$, we obtain decaying turbulence in which thin current sheets form and decay. For increasing values of a, the turbulence changes character, driven by the source of free energy stored in the mean fields. Consequently, the thin current sheets form and persist for longer times.

For $a = 0$, the fluctuations p and v, which are initially zero, remain zero for all times since they are passively transported by the RMHD equations. For $a \neq 0$, their root mean square (rms) value increase to a nonzero level that rises with the value of a. Figure 6 shows the level of $p_{\rm rms}$ in the quasi-saturated state (*diamonds*) as a function of M for different values of a, with $M(t = 0) \approx 0.01$. In order to quantify the approximate saturation level of the fluctuations, two lines are drawn: a solid line corresponding to the level $p_{\rm rms} = M$, and a dashed line corresponding to the level $p_{\rm rms} = M^2$. We note that saturated values of $p_{\rm rms}$ approach the line $p_{\rm rms} = M$ as the parameter a increases. Even for values of a as small as 0.04, the condition $p_{\rm rms} = M$ is attained. This trend persists for higher values of a. To demonstrate that similar qualitative features also appear for higher initial values of M, we show data from runs with $M(t = 0) \approx 0.1$ (*stars*).

Note that when a is small enough ($\leq 10^{-4}$) the quasi-saturated level of the pressure fluctuation lies below the $p_{\rm rms} = M^2$ line. This implies that the contribution from p_1 to the total pressure fluctuation may actually become subdominant to the second order contribution p_2. In the small a limit, we thus recover ZM's result that the pressure fluctuations are second order.

Figure 7 shows the parallel flow attains parity with $p_{\rm rms}$ for $a \geq 0.01$. The dynamical coupling of the parallel flow with pressure fluctuations in the presence of inhomogeneities is one of the significant new features of four-field MHD that is absent in RMHD.

We recall that all the runs are initialized with initial magnetic energy much smaller than initial flow energy. It is of interest to examine the role that inhomogeneities play in driving the system to equipartition, with $E_M = E_K$. This is the subject of Figure 8, where it is seen that values of a larger than 0.06 are sufficient to bring the system to the $E_M = E_K$ line. The equipartition of kinetic and magnetic energy is a manifestation of the so-called Alfvén effect which represents the tendency of alignment (or anti-alignment) of the velocity and magnetic field fluctuations in incompressible MHD turbulence (Pouquet, Frisch, & Leorat 1976; Dobrowolny, Mangeney, & Veltri 1980; Biskamp 1993; Zweibel & McKee 1995; Bhattacharjee & Yuan 1995; Lau & Siregar 1996). Our numerical results demonstrate that this tendency persists in weakly compressible, four-field MHD when the effect of inhomogeneities is included, and the turbulence is driven by fixed mean fields. We find, furthermore, that this tendency of equipartition also extends to thermal fluctuations.

5. SUMMARY AND IMPLICATIONS FOR OBSERVATIONS

To describe low Mach number compressible turbulence in a $\beta \leq 1$ plasma permeated by a magnetic field, we have obtained a new four-field system of equations (18)–(21) by asymptotic reduction of the compressible resistive MHD equations. These equations include the effects of spatial inhomogeneity in the mean fields. We call this system weakly compressible because the velocity fluctuation obeys a two-dimensional incompressibility condition akin to the Proudman-Taylor theorem in hydrodynamics.

The four-field system represents a rigorous generalization of RMHD (which is a two-field system for $\beta \ll 1$ plasmas) or the nearly incompressible system of ZM. We have shown that both RMHD or nearly incompressible MHD can be derived as special cases of the four-field system either by taking the $\beta \ll 1$ limit or by neglecting all inhomogeneities in the mean fields. In a spatially inhomogeneous $\beta \sim 1$ plasma, the four-field variables—magnetic flux, parallel vorticity, pressure, and parallel flow—are strongly coupled to each other. Then compressibility enters the dynamics at leading order and it cannot be claimed that the compressible fluctuations can be enslaved to a two-dimensional incompressible flow field. In the four-field system, the first-order pressure or density fluctuations evolve to nonzero values even if they are chosen to be zero initially, and even modest inhomogeneities are enough to raise the level of these fluctuations to the Mach number of the turbulence.

We have presented two-dimensional numerical results for the four-field system to quantify the effect of spatial inhomogeneities. We find that inhomogeneities have a significant effect on the magnitude and spatio-temporal structure of current (as well as vortex) sheets. The turbulence is driven by the free energy contained in the spatially inhomogeneous mean profiles, and the system attains equipartition in the four-field variables.

Some qualitative features of the four-field model are in accord with observations of compressible solar wind turbulence. Based on a large data set of *Voyager* observations between 1 and 7 AU, it has been pointed out that density fluctuations, which are proportional to pressure fluctuations for an isothermal plasma, do not generally scale as M^2 as required by the nearly incompressible model of Zank & Matthaeus (1993), (Tu & Marsch 1994; Bavassano, Bruno, & Klein 1995). Rather, the data seems to suggest the presence of an $O(M)$ scaling that is qualitatively consistent with the numerical evidence from the four-field model when the background is spatially inhomogeneous. Furthermore, there appears to be substantial observational evidence for equipartition of energy between magnetic, kinetic, and thermal fluctuations when $\beta \sim 1$ (see Tu & Marsch 1995). Our numerical results based on the four-field equations suggest that the presence of spatial inhomogeneities provide a natural mechanism for the attainment of equipartition in driven turbulence.

Much more work remains to be done. An outstanding question, not addressed in this paper, is the form of the turbulent energy spectrum. Even for incompressible MHD turbulence mediated by the weak interaction of shear-Alfvén waves in a spatially uniform background magnetic field, the precise nature of wave-wave interactions and the form of the energy spectrum is a subject of active debate (Sridhar & Goldreich 1994; Montgomery & Matthaeus 1995; Ng & Bhattacharjee 1996, 1997; Chen & Kraichnan 1997). However, all the cited studies do agree that the energy spectrum is strongly anisotropic in the presence of a uniform magnetic field. Evidence for anisotropic turbulence is one of the strongest results from radio wave scintillation studies of heliospheric and interstellar turbulence. Radio wave scattering in the solar wind close to the Sun is highly anisotropic, with the "long axis" of the irregularities being in the radial, magnetic field-oriented direction and with axial ratios in excess of 10:1 (Armstrong et al. 1990; Grall et al. 1997). Anisotropic scattering, indicative of anisotropic irregularities, is also a general characteristic of interstellar scattering (Wilkinson, Narayan, & Spencer 1994; Frail et al. 1994; Molnar et al. 1995). The observed ratios are smaller than in the heliospheric case, but this may be due to averaging by integration along the line of sight. It seems likely that the axial ratio of the density irregularities exceed the maximum observed factors of 4:1 (Frail et al. 1994). In any case, the existence of such anisotropy in both heliospheric and interstellar plasmas suggests turbulence of the sort described in this paper. We have shown in § 4 that if the magnetic field is spatially uniform, the four-field equations reduce to RMHD for which the anisotropic spectrum (in the limit of weak turbulence) has been discussed elsewhere (Ng & Bhattacharjee 1996, 1997). In future work, we propose to extend our RMHD results to weakly compressible four-field MHD turbulence, including in the theory the effect of spatial inhomogeneities.

APPENDIX

DERIVATION OF THE FOUR-FIELD EQUATIONS

We derive the four-field equations from the compressible resistive MHD equations (1)–(4) or, equivalently, equations (10), (6b), (3), and (12), obtained after the scaling discussed in § 2. We consider the asymptotic expansion scheme (7), where the subscripts on the quantities denote their order in the small parameter ϵ. We assume that $\nabla_{\|} \sim O(1)$, $\nabla_{\perp} \sim O(1/\epsilon)$ and $\partial/\partial t \sim O(1)$ when they operate on the first-order quantities, while $\nabla \sim O(1)$ and $\partial/\partial t \sim O(\epsilon^2)$ when they operate on the zero-order quantities.

From $O(1)$ of the conditions $\nabla \cdot \boldsymbol{B} = 0$ and $\nabla \cdot \boldsymbol{B}_0 = 0$, we obtain equation (13). From $O(1)$ of equation (10), we find

$$\nabla p_0 - (\nabla \times \boldsymbol{B}_0) \times \boldsymbol{B}_0 + \nabla_{\perp} p_1 - (\nabla_{\perp} \times \boldsymbol{B}_1) \times \boldsymbol{B}_0 = 0 \,.$$

Using the magnetostatic equilibrium condition (11), we obtain

$$\nabla_{\perp}(p_1 + \boldsymbol{B}_0 \cdot \boldsymbol{B}_1) = O(\epsilon) \,,$$

which yields equation (14) to $O(\epsilon^2)$.

From $O(1)$ of equation (12), we obtain equation (16). Therefore, we can represent the first-order magnetic and velocity fields in the forms (15) and (17), respectively. Note that A and ϕ are of the order $O(\epsilon^2)$, and p_1, and v_1 are $O(\epsilon)$. From equations (4) and (5a), with the assumption that $\eta \sim O(\epsilon^2)$ (consistent with Kruskal's principle of maximal balance or minimal simplification), we obtain

$$p = \rho^{\gamma} + O(\epsilon^2) \,.$$

From the $O(1)$ and $O(\epsilon)$ terms of the equation above, we obtain

$$p_0 = \rho_0^{\gamma} \,, \qquad p_1 = \gamma \rho_0^{\gamma - 1} \rho_1 \,.$$

Thus, we need only to solve four dynamical equations for the four-field quantities A, ϕ, p_1, and v_1.

Keeping terms up to $O(\epsilon)$, equation (2) becomes

$$\frac{\partial \boldsymbol{B}_1}{\partial t} + \nabla \times (\boldsymbol{B}_0 \times \boldsymbol{v}_1) + \nabla_{\perp} \times (\boldsymbol{B}_1 \times \boldsymbol{v}_1) + \boldsymbol{B}_0 \nabla_{\perp} \cdot \boldsymbol{v}_2 + \eta \nabla_{\perp} \times \nabla_{\perp} \times \boldsymbol{B}_1 = O(\epsilon^2) \,. \tag{A1}$$

The following relations hold:

$$\frac{\partial \boldsymbol{B}_1}{\partial t} = \nabla_\perp \frac{\partial A}{\partial t} \times \boldsymbol{b} - \frac{\partial p_1}{\partial t} \boldsymbol{b} + O(\epsilon^2) , \qquad \nabla \times (\boldsymbol{B}_0 \times \boldsymbol{v}_1) = -\nabla_\perp(\boldsymbol{B}_0 \cdot \nabla\phi) \times \boldsymbol{b} + O(\epsilon^2) ,$$

$$\nabla_\perp \times (\boldsymbol{B}_1 \times \boldsymbol{v}_1) = -\nabla_\perp(\nabla_\perp \phi \times \nabla_\perp A \cdot \boldsymbol{b}) \times \boldsymbol{b} + (\boldsymbol{B}_1 \cdot \nabla_\perp v_1 - \boldsymbol{v}_1 \cdot \nabla_\perp p_1)\boldsymbol{b} + O(\epsilon^2) ,$$

$$\eta \nabla_\perp \times \nabla_\perp \times \boldsymbol{B}_1 = -\eta[\nabla_\perp(\nabla_\perp^2 A) \times \boldsymbol{b} + (\nabla_\perp^2 p_1)\boldsymbol{b}] + O(\epsilon^2) .$$

Taking the cross product of equation (A1) with $\boldsymbol{B}_0$, we obtain

$$\nabla_\perp\left(\frac{\partial A}{\partial t} - \boldsymbol{B}_0 \cdot \nabla\phi - \nabla_\perp \phi \times \nabla_\perp A \cdot \boldsymbol{b} - \eta\nabla_\perp^2 A\right) = 0 .$$

Equation (18) then follows from the definitions (eqs. [17], [22d]) and standard boundary conditions on the fields. Taking the dot product of equation (A1) with $\boldsymbol{B}_0$, we obtain

$$-\frac{dp_1}{dt} + B_0^2(\nabla \cdot \boldsymbol{v}_1 + \nabla_\perp \cdot \boldsymbol{v}_2) - \boldsymbol{v}_1 \cdot \nabla p_0 + 2\boldsymbol{v}_1 \cdot \nabla P + Dv_1 + \eta \nabla_\perp^2 p_1 = 0 , \tag{A2}$$

where we have used the definitions (22c)–(22f) as well as the identity

$$B_0^2 \nabla \cdot \boldsymbol{v}_1 = -\boldsymbol{v}_1 \cdot \nabla(p_0 + B_0^2) - \boldsymbol{B}_0 \cdot \nabla v_1 + O(\epsilon^2) ,$$

which follows from equation (11) and (17). On the other hand, the $O(\epsilon)$ term of equation (12) yields

$$\frac{dp_1}{dt} + \gamma p_0(\nabla \cdot \boldsymbol{v}_1 + \nabla_\perp \cdot \boldsymbol{v}_2) + \boldsymbol{v}_1 \cdot \nabla p_0 = 0 . \tag{A3}$$

We now subtract γp_0 times equation (A2) from B_0^2 times equation (A3) to obtain equation (20). Taking the dot product of equation (10) with $\boldsymbol{B}_0$, we obtain

$$\rho_0 \frac{d(\boldsymbol{B}_0 \cdot \boldsymbol{v}_1)}{dt} + \boldsymbol{B}_0 \cdot \{\nabla p_1 - [(\nabla \times \boldsymbol{B}_0 + \nabla_\perp \times \boldsymbol{B}_1) \times \boldsymbol{B}_1]\} = O(\epsilon^2) .$$

It can be shown that

$$\boldsymbol{B}_0 \cdot [(\nabla \times \boldsymbol{B}_0) \times \boldsymbol{B}_1] = -\boldsymbol{B}_1 \cdot \nabla p_0 + O(\epsilon^2) , \qquad \boldsymbol{B}_0 \cdot [(\nabla_\perp \times \boldsymbol{B}_1) \times \boldsymbol{B}_1] = -\boldsymbol{B}_1 \cdot \nabla_\perp p_1 + O(\epsilon^2) .$$

Then, with the help of equation (17), we obtain equation (21). Taking the curl of equation (10), we obtain

$$\rho\left[\frac{\partial \boldsymbol{\Omega}}{\partial t} + \nabla \times (\boldsymbol{\Omega} \times \boldsymbol{v})\right] + \nabla\rho \times \left(\frac{\partial}{\partial t} + \boldsymbol{v} \cdot \nabla\right) \times [(\nabla \times \boldsymbol{B}) \times \boldsymbol{B}] = 0 , \tag{A4}$$

where $\boldsymbol{\Omega} = \nabla \times \boldsymbol{v}$. We have

$$\Omega_0 = \nabla \times \boldsymbol{v}_1 = -\nabla_\perp v_1 \times \boldsymbol{b} - (\nabla_\perp^2 \phi)\boldsymbol{b} .$$

Only the first and third terms in equation (A4) contribute to the $O(1)$ term. Thus, we obtain

$$\rho_0\left(\frac{\partial \boldsymbol{\Omega}_0}{\partial t} + \boldsymbol{v}_1 \cdot \nabla_\perp \Omega_0 - \Omega_0 \cdot \nabla_\perp \boldsymbol{v}\right) = (\boldsymbol{B}_0 \cdot \nabla + \boldsymbol{B}_1 \cdot \nabla_\perp)\nabla_\perp \times \boldsymbol{B}_1 - (\nabla \times \boldsymbol{B}_0 + \nabla_\perp \times \boldsymbol{B}_1) \cdot \nabla_\perp \boldsymbol{B}_1 - \nabla_\perp \times \boldsymbol{B}_1 \cdot \nabla \boldsymbol{B}_0 , \tag{A5}$$

where we have used the identity

$$\boldsymbol{B}_0 \cdot \nabla\nabla \times \boldsymbol{B}_0 - (\nabla \times \boldsymbol{B}_0) \cdot \nabla \boldsymbol{B}_0 = 0 ,$$

which can be deduced from equation (11). We take the dot product of equation (A5) with $\boldsymbol{B}_0$ and use the following relations:

$$\boldsymbol{B}_0 \cdot \frac{\partial \Omega_0}{\partial t} = \frac{\partial \Omega}{\partial t} + O(\epsilon) , \qquad \boldsymbol{v}_1 \cdot \nabla_\perp \Omega_0 \cdot \boldsymbol{B}_0 = \boldsymbol{v}_1 \cdot \nabla_\perp \Omega + O(\epsilon) , \qquad -\Omega_0 \cdot \nabla_\perp \boldsymbol{v} \cdot \boldsymbol{B}_0 = \boldsymbol{\Omega}_0 \cdot \nabla_\perp v_1 + O(\epsilon) = O(\epsilon) ,$$

$$\boldsymbol{B}_0 \cdot \nabla(\nabla_\perp \times \boldsymbol{B}_1) \cdot \boldsymbol{B}_0 = \boldsymbol{B}_0 \cdot \nabla J - (\boldsymbol{B}_0 \cdot \nabla \boldsymbol{B}_0) \cdot \nabla_\perp \times \boldsymbol{B}_1 + O(\epsilon) , \qquad \boldsymbol{B}_1 \cdot \nabla_\perp(\nabla_\perp \times \boldsymbol{B}_1) \cdot \boldsymbol{B}_0 = \boldsymbol{B}_1 \cdot \nabla_\perp J + O(\epsilon) ,$$

$$-(\nabla \times \boldsymbol{B}_0 + \nabla_\perp \times \boldsymbol{B}_1) \cdot \nabla_\perp \boldsymbol{B}_1 \cdot \boldsymbol{B}_0 = (\nabla \times \boldsymbol{B}_0 + \nabla_\perp \times \boldsymbol{B}_1) \cdot \nabla_\perp p_1 + O(\epsilon) ,$$

$$-\nabla_\perp \times \boldsymbol{B}_1 \cdot \nabla \boldsymbol{B}_0 \cdot \boldsymbol{B}_0 = -\nabla_\perp \times \boldsymbol{B}_1 \cdot \nabla(B_0^2/2) + O(\epsilon) ,$$

Then equation (A5) becomes

$$\rho_0 \frac{d\boldsymbol{\Omega}}{dt} = DJ - \nabla_\perp \times \boldsymbol{B}_1 \cdot \left(\boldsymbol{B}_0 \cdot \nabla \boldsymbol{B}_0 + \frac{\nabla B_0^2}{2}\right) + (\nabla \times \boldsymbol{B}_0 + \nabla_\perp \times \boldsymbol{B}_1) \cdot \nabla_\perp p_1 ,$$

which reduces to equation (19) if we note that

$$\nabla_\perp \times \boldsymbol{B}_1 \cdot (\boldsymbol{B}_0 \cdot \nabla \boldsymbol{B}_0 + \nabla B_0^2/2) = (\boldsymbol{b} \cdot \nabla B_0^2) J - \boldsymbol{b} \times \nabla(p_0 + B_0^2) \cdot \nabla_\perp p_1 ,$$

$$\nabla \times \boldsymbol{B}_0 \cdot \nabla_\perp p_1 = (\boldsymbol{b} \times \nabla p_0) \cdot \nabla_\perp p_1 ,$$

$$\nabla_\perp \times \boldsymbol{B}_1 \cdot \nabla_\perp p_1 = 0 .$$

Thus, we obtain the four-field equations (18)–(21).

REFERENCES

Armstrong, J. W., Coles, W. A., Kojima, K., & Rickett, B. J. 1990, ApJ, 358, 685
Batchelor, G. K. 1979, An Introduction to Fluid Dynamics (Cambridge: Cambridge Univ. Press)
Bavassano, B., Bruno, R., & Klein, L. W. 1995, J. Geophys. Res., 100, 5871
Bhattacharjee, A., & Hameiri, E. 1988, Phys. Fluids, 31, 1153
Bhattacharjee, A., & Yuan, Y. 1995, ApJ, 449, 739
Biskamp, D. 1993, Nonlinear Magnetohydrodynamics (Cambridge: Cambridge Univ. Press)
Chen, S., & Kraichnan, R. H. 1997, J. Plasma Phys., 57, 187
Dahlquist, G., Björck, A., & Anderson, N. 1974, Numerical Methods (Englewood Cliffs, NJ: Prentice-Hall)
Dobrowolny, M., Mangeney, A., & Veltri, P. 1980, Phys. Rev. Lett., 45, 144
Frail, D. A., Diamond, P. J., Cordes, J. M., & Van Langevelde, H. J. 1994, ApJ, 427, L43
Gammie, C. F., & Ostriker, E. C. 1996, ApJ, 466, 814
Grall, R. R., Coles, W. A., Spangler, S. R., Sakurai, T., & Harmon, J. K. 1997, J. Geophys. Res., 102, 263
Kruskal, M. D. 1963, in Mathematical Models in Physical Sciences, ed. S. Drobot & P. A. Viebrock (Englewood Cliffs, NJ: Prentice Hall), 17
Lau, Y.-T., & Siregar, E. 1996, ApJ, 465, 451
Malara, F., Primavera, L., & Veltri, P. 1996, J. Geophys. Res., 101, 21597
Matthaeus, W. H., & Brown, M. 1988, Phys. Fluids, 31, 3634
Molnar, L. A., Mutel, R. L., Reid, M. J., & Johnston, K. J. 1995, ApJ, 438, 708
Montgomery, D., Brown, M., & Matthaeus, W. 1987, J. Geophys. Res., 92, 282
Montgomery, D., & Matthaeus, W. H. 1995, ApJ, 447, 706
Ng, C. S., & Bhattacharjee, A. 1996, ApJ, 465, 845
———. 1997, Phys. Plasmas, 4, 605
Passot, T., Vázquez-Semadini, E., & Pouquet, A. 1995, ApJ, 455, 536
Pouquet, A., Frisch, U., & Leorat, J. 1976, J. Fluid Mech., 77, 321
Roberts, D. A., Ghosh, S., & Goldstein, M. L. 1996, Geophys. Res. Lett., 23, 591
Rosenbluth, M. N., Monticello, D. A., Strauss, H. R., & White, R. B. 1976, Phys. Fluids, 19, 1987
Sridhar, S., & Goldreich, P. 1994, ApJ, 432, 612
Strauss, H. R. 1976, Phys. Fluids, 19, 134
Tu, C.-Y., & Marsch, E. 1994, J. Geophys. Res., 99, 21, 481
———. 1995, Space Sci. Rev., 73, 1
Wilkinson, P. N., Narayan, R., & Spencer, R. E. 1994, MNRAS, 269, 67
Zank, G. P., & Matthaeus, W. H. 1992, J. Plasma Phys., 48, 85
———. 1993, Phys. Fluids, A5, 257
Zweibel, E. G., & McKee, C. F. 1995, ApJ, 439, 779